

Trong Kien Nguyen¹

Combination of feedback control and spring-damper to reduce the vibration of crane payload

Operating cranes is challenging because payloads can experience large and dangerous oscillations. Anti-sway control of crane payload can be approached by the active methods, such as feedback control, or passive methods. The feedback control uses the feedback measurement of swing vibration to produce the command sent to a motor. The feedback control shows good effectiveness, but conflict with the actions of the human operator is a challenge of this method. The passive method uses the spring-damper to dissipate energy. The passive method does not cause conflict with the human operator but has limited performance. This paper presents the combination of two methods to overcome the disadvantages of each separate one. The passive method is used to improve the efficiency of the feedback method to avoid conflicts with the human operator. The effectiveness of the combination is simulated in a 2D crane model.

1. Introduction

The crane payload suspended by cables is highly flexible. External disturbances, such as wind or motion of the support unit (e.g., the bridge or trolley, or tower), can cause the residual sway oscillation. These residual sways reduce the crane's operating speed, affect the durability of the cable, and cause a danger. Since the crane is a popular device, reducing swaying vibrations for the payload is extremely valuable.

The anti-swing control strategy proposed in the literature is often carried out by active method including open- and closed-loop control. The closed-loop (feedback) techniques use the crane measurements such as swing angle to provide control commands [1–5]. On the other hand, the open-loop (feedforward) techniques,

✉ Trong Kien Nguyen, e-mail: nguyentrongkien82@gmail.com

¹Faculty of Civil Engineering, Vinh University, Vinh City, Nghe An, Vietnam.



modify the command before sending it to the crane motors [6]. Besides, some recent studies applied passive systems to control the payload oscillation [7, 8]. A typical passive system is the radial spring-damper, which provides nonlinear Coriolis damping for anti-sway crane control [8].

Both the active method and the method using radial spring-damper mentioned above have certain disadvantages. Regarding the active feedback method, it can effectively control payload swing under the influence of human operator commands and external disturbances. However, most cranes are controlled by a human. They are controlled in real-time by human operators that provide not only the initial reference command to the crane, but also issue additional commands as necessary to maneuver the crane through the desired trajectory. Any additional input from a computerized feedback controller can adversely conflict with the input from the human operator [9–11]. Therefore, a feedback control must have low authority to avoid conflicts. In other words, the feedback gain should be not too large, but this limits the real effectiveness of the feedback control. Another active method of reducing crane payload oscillation employs feedforward techniques. The input shaping, a typical feedforward technique, is implemented by convolving a series of impulses, called the input shaper, with the reference command [11–13]. Although it does not require the sensors, the input shaping cannot counteract external disturbances due to its open-loop nature [14, 15]. The passive method, conversely, has limited performance but can counteract external disturbances and does not conflict with the crane operator.

From the above analysis we see that: to avoid conflict between the feedback control and the crane operator, the feedback control must have a low impact on the system, but this reduces its efficiency. Therefore, we can combine feedback control with the input shaping or combine feedback control with the spring-damper to improve the efficiency of feedback control. This is explained as follows. If the feedback control is combined with the input shaping, then significant work has been directed at input shaping to reduce operator-induced vibration, significantly less effort has been placed on combining input shaping with feedback control to suppress external disturbances. If the feedback control is combined with the spring-damper, it can be used as the secondary system and is expected to improve the feedback control. Each method gives a small effect combined for a larger effect. The combination of feedback control and input shaping has been presented in [14, 15]. However, since these are active methods, more control is required, thus increasing the delay time and making the system more complex. The contribution of this paper is to propose combining the feedback control method with the spring-damper to improve the efficiency of the feedback control. Payload oscillations are eliminated by a low-authority feedback controller that is designed to operate "in the background" without disturbing the human operator. At the same time, the spring-damper also contributes a part to reducing these oscillations.

The next section presents the dynamic model of a 2D crane. In Section 3, the optimal parameters of radial spring-damper have been derived. Then, the effec-

tiveness of the proposed approach is verified numerically, in Section 4. Finally, Section 5 demonstrates the effectiveness of the combined method by the software RECURDYN.

2. Mathematical model

The model of the combination of feedback control and spring-damper to reduce a 2D crane sway motion is shown in Fig. 1.

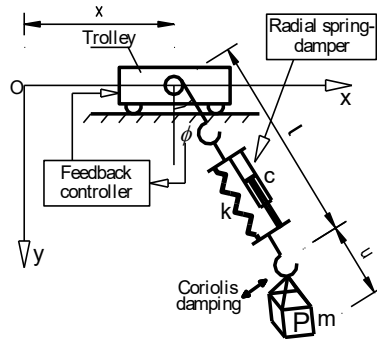


Fig. 1. Combination of feedback control and passive radial spring and damper

In Fig. 1, the following simplified assumptions have been made:

- There is only the trolley motion's command.
- The spring and damper weights are ignored in comparison with the payload weight, so that the single pendulum can be used to model the system.

Table 1.

Notations in Fig. 1

| Symbol | Description |
|-----------------------------------|---|
| m | Payload mass |
| k, c | Spring's stiffness and damper's coefficient |
| ϕ | Payload swing angle |
| l | Distances between the trolley and the payload in the static condition |
| u | Radial motion of payload measured from static position |
| $u_0 = mg/k$ | Static deflection of spring |
| x | Trolley displacement |
| g | Acceleration of gravity |
| $\omega_s = \sqrt{g/l}$ | Natural frequency of pendulum |
| $\tau = \omega_s t$ | Non-dimensional time |
| $r = \frac{\sqrt{k/m}}{\omega_s}$ | Ratio between natural frequencies |
| $\zeta = \frac{c}{2m\omega_s}$ | Damping ratios of damper |
| $u_n = u/l, x_n = x/l$ | Non-dimensional forms of radial movement and trolley movement |

- The cable's stiffness is large enough in comparison with the spring stiffness, so that the cable deformation can be ignored.

With those three simplifications, to write the motion equations, we introduce the symbols that are shown and explained in Table 1.

Based on the coordinate system in Fig. 1, with the horizontal position of the trolley as x , the position of the payload (x_P , y_P) is obtained as:

$$\begin{aligned} x_P &= x + (l + u) \sin \phi, \\ y_P &= (l + u) \cos \phi. \end{aligned} \quad (1)$$

The dynamic model for this 2D crane is derived by using the Lagrange method. After some manipulations, two Lagrange equations of motion reduce to:

$$\begin{aligned} 2\dot{u}\dot{\phi} + \ddot{x} \cos \phi + \ddot{\phi} (l + u) + g \sin \phi &= 0, \\ m\ddot{x} \sin \phi + m\ddot{u} + ku + c\dot{u} + mg (1 - \cos \phi) - m\dot{\phi}^2 (l + u) &= 0. \end{aligned} \quad (2)$$

Using some non-dimensional parameters in Table 1, we reduce the Eq. (2) to the non-dimensional form as follows. Dividing both sides of the first equation in (2) by l and dividing both sides of the second equation in (2) by ml we have

$$\begin{aligned} 2\frac{\dot{u}}{l}\dot{\phi} + \frac{\ddot{x}}{l} \cos \phi + \ddot{\phi} \left(1 + \frac{u}{l}\right) + \frac{g}{l} \sin \phi &= 0, \\ \frac{\ddot{x}}{l} \sin \phi + \frac{\ddot{u}}{l} + \frac{k}{m} \frac{u}{l} + \frac{c}{m} \frac{\dot{u}}{l} + \frac{g}{l} (1 - \cos \phi) - \dot{\phi}^2 \left(1 + \frac{u}{l}\right) &= 0, \end{aligned} \quad (3)$$

or

$$\begin{aligned} 2\frac{\dot{u}}{l}\dot{\phi} + \frac{\ddot{x}}{l} \cos \phi + \ddot{\phi} \left(1 + \frac{u}{l}\right) + \omega_s^2 \sin \phi &= 0, \\ \frac{\ddot{x}}{l} \sin \phi + \frac{\ddot{u}}{l} + r^2 \omega_s^2 \frac{u}{l} + 2\zeta \omega_s \frac{\dot{u}}{l} + \omega_s^2 (1 - \cos \phi) - \dot{\phi}^2 \left(1 + \frac{u}{l}\right) &= 0. \end{aligned} \quad (4)$$

As we use the non-dimensional time in Table 1, from now, the dot operator denotes the differentiation to the normalized time τ , so we have

$$\begin{aligned} 2\dot{u}_n \dot{\phi} \omega_s^2 + \ddot{x}_n \omega_s^2 \cos \phi + \ddot{\phi} \omega_s^2 (1 + u_n) + \omega_s^2 \sin \phi &= 0, \\ \ddot{x}_n \omega_s^2 \sin \phi + \ddot{u}_n \omega_s^2 + r^2 \omega_s^2 u_n + 2\zeta \omega_s \omega_s \dot{u}_n + \omega_s^2 (1 - \cos \phi) - \dot{\phi}^2 \omega_s^2 (1 + u_n) &= 0. \end{aligned} \quad (5)$$

Dividing both sides of the equation in (5) by ω_s^2 gives the final equation used in simulation:

$$\begin{aligned} 2\dot{u}_n \dot{\phi} + \ddot{x}_n \cos \phi + \ddot{\phi} (1 + u_n) + \sin \phi &= 0, \\ \ddot{x}_n \sin \phi + \ddot{u}_n + r^2 u_n + 2\zeta \dot{u}_n + 1 - \cos \phi - \dot{\phi}^2 (1 + u_n) &= 0. \end{aligned} \quad (6)$$

3. Combining feedback control and radial spring-damper

We consider the simple feedback control which has low authority. As said above, the feedback control system must have low authority to avoid conflict with the crane operator. The low authority feedback control allows the crane operator to control the operation and does not make unexpected motions that surprise and frustrate the human operator. Therefore, we choose the simple controller as a proportional controller. Using the proportional (P) controller, we have the velocity control command in the form:

$$\dot{x}_n = \beta\phi \quad (7)$$

in which β is the control gain.

To obtain the analytical solution of the optimal parameters, we approximate the motion equations in (6) by Taylor expansion of the trigonometric functions to the second-order, that:

$$\sin \phi \approx \phi; \quad \cos \phi \approx 1 - \frac{\phi^2}{2}. \quad (8)$$

Moreover, the normalized displacement u_n is assumed to be small in comparison with the unity, so that

$$1 + u_n \approx 1. \quad (9)$$

Eq. (6) with the approximations (8), (9) are combined with the controller (7) to be rewritten as follows:

$$\begin{aligned} 2\dot{u}_n\dot{\phi} + \ddot{\phi} + \phi + \beta\dot{\phi} &= 0, \\ \ddot{u}_n + r^2u_n + 2\zeta\dot{u}_n + \frac{\phi^2}{2} - \dot{\phi}^2 + \beta\dot{\phi}\phi &= 0. \end{aligned} \quad (10)$$

Optimization of the damper parameters when combined

To perform a linearization equivalent to the Coriolis term, we replace the Coriolis term by the effective damping:

$$\dot{u}_n\dot{\phi} \rightarrow \zeta_e\dot{\phi}, \quad (11)$$

in which the effective damping ζ_e is found by minimizing the following error:

$$\zeta_e = \frac{\langle \dot{u}_n\dot{\phi}^2 \rangle}{\langle \dot{\phi}^2 \rangle}. \quad (12)$$

In the case of free oscillation (but with feedback control), we consider the average operator in the form of the integral from 0 to infinity.

$$\zeta_e = \frac{\int_0^{\infty} \dot{u}_n\dot{\phi}^2 d\tau}{\int_0^{\infty} \dot{\phi}^2 d\tau}. \quad (13)$$

Substituting $\dot{u}_n \dot{\phi}$ by $\zeta_e \dot{\phi}$ in (10) and writing the equations in a matrix form we get:

$$\dot{\mathbf{q}} = \mathbf{A} \mathbf{q} \quad (14)$$

where \mathbf{q} is the expanded state vector and \mathbf{A} is the system matrix determined by:

$$\begin{aligned} \mathbf{q} &= \left[q_1 \quad q_2 \quad q_3 \quad q_4 \quad q_5 \quad q_6 \quad q_7 \right]^T \\ &= \left[\phi \quad \dot{\phi} \quad u_n \quad \dot{u}_n \quad \phi^2 \quad \dot{\phi}^2 \quad \phi \dot{\phi} \right]^T, \\ \mathbf{q}|_{\tau=0} &= \left[\phi_0 \quad 0 \quad 0 \quad 0 \quad \phi_0^2 \quad 0 \quad 0 \right]^T, \\ \mathbf{A} &= \begin{bmatrix} \mathbf{A}_1 & \mathbf{0}_{2 \times 5} \\ \mathbf{0}_{5 \times 2} & \mathbf{A}_2 \end{bmatrix}, \quad \mathbf{A}_1 = \begin{bmatrix} 0 & 1 \\ -1 & -2\zeta_e - \beta \end{bmatrix}, \\ \mathbf{A}_2 &= \begin{bmatrix} 0 & 1 & 0 & 0 & 0 \\ -r^2 & -2\zeta & -1/2 & 1 & -\beta \\ 0 & 0 & 0 & 0 & 2 \\ 0 & 0 & 0 & -4\zeta_e - 2\beta & -2 \\ 0 & 0 & -1 & 1 & -2\zeta_e - \beta \end{bmatrix}. \end{aligned} \quad (15)$$

The effective damping Eq. (13) is rewritten as:

$$\zeta_e = \frac{\int_0^{\infty} q_4 q_6 d\tau}{\int_0^{\infty} q_2^2 d\tau}. \quad (17)$$

We use the conditions of double poles [16] to give optimal conditions and obtain the analytical forms of the optimal parameters. The two dimensionless parameters that need to be optimized are r and ζ . Because r and ζ only appear in the matrix \mathbf{A}_2 , the characteristic polynomial of \mathbf{A}_2 is determined by:

$$P_{A_2}(s) = (s + 2\zeta_e + \beta) \left[s^2 + (4\zeta_e + 2\beta) s + 4 \right] \left(s^2 + 2\zeta s + r^2 \right). \quad (18)$$

The quintic polynomial Eq. (13) has one real root and two pairs of complex conjugate roots. The repeated roots conditions give:

$$r = 2, \quad (19)$$

$$\zeta = 2\zeta_e + \beta. \quad (20)$$

Substituting Eqs. (19), (20) into Eq. (16), we have the linear system depending on the effective damping ζ_e . The next step is to calculate the effective damping from

Eq. (17). It is well known that, in the linear system Eq. (14), the infinite integrals of the quadratic form in Eq. (17) can be obtained by solving the Lyapunov matrix equations. A general infinite integral of the quadratic form is given by:

$$J = \int_0^{\infty} \mathbf{q}^T \mathbf{Q} \mathbf{q} d\tau \quad (21)$$

where \mathbf{Q} is a positive definite matrix.

Let us consider the matrix \mathbf{P} being the solution of the Lyapunov matrix equation as:

$$\mathbf{P} \mathbf{A} + \mathbf{A}^T \mathbf{P} + \mathbf{Q} = \mathbf{0}. \quad (22)$$

Substituting Eq. (22) into the integral Eq. (21) and using the state space Eq. (14) gives:

$$\begin{aligned} J &= \int_0^{\infty} \mathbf{q}^T \mathbf{Q} \mathbf{q} d\tau = - \int_0^{\infty} \mathbf{q}^T (\mathbf{P} \mathbf{A} + \mathbf{A}^T \mathbf{P}) \mathbf{q} d\tau \\ &= - \int_0^{\infty} (\mathbf{q}^T \mathbf{P} \dot{\mathbf{q}} + \dot{\mathbf{q}}^T \mathbf{P} \mathbf{q}) d\tau = (\mathbf{q}^T \mathbf{P} \mathbf{q}) \Big|_0^{\infty} \\ &= \mathbf{q}_0^T \mathbf{P} \mathbf{q}_0 - \mathbf{q}(\infty)^T \mathbf{P} \mathbf{q}(\infty) = \mathbf{q}_0^T \mathbf{P} \mathbf{q}_0, \end{aligned} \quad (23)$$

in which \mathbf{q}_0 is a vector containing the initial conditions and $\mathbf{q}(\infty) = \mathbf{0}$ with the assumption that the system is asymptotically stable due to the presence of damping.

Using Eqs. (22) and (23) in Eq. (17), after a few computational steps, we obtain:

$$\int_0^{\infty} q_4 q_6 d\tau = \int_0^{\infty} \dot{u}_n \phi^2 d\tau = \frac{-3\phi_0^4 \left(\begin{array}{l} 48\zeta_e^4 + 144\beta\zeta_e^3 - 36\zeta_e^2 + 144\beta^2\zeta_e^2 \\ +60\beta^3\zeta_e - 36\beta\zeta_e - 9\beta^2 - 4 + 9\beta^4 \end{array} \right)}{32(2\zeta_e + \beta)^2 (12\zeta_e^2 + 12\beta\zeta_e + 4 + 3\beta^2)^2}, \quad (24)$$

$$\int_0^{\infty} q_2^2 d\tau = \int_0^{\infty} \phi^2 d\tau = \frac{\phi_0^2}{2(2\zeta_e + \beta)}. \quad (25)$$

Equation (17) is rewritten to:

$$\zeta_e = \frac{-3\phi_0^2 \left(\begin{array}{l} 48\zeta_e^4 + 144\beta\zeta_e^3 - 36\zeta_e^2 + 144\beta^2\zeta_e^2 \\ +60\beta^3\zeta_e - 36\beta\zeta_e - 9\beta^2 - 4 + 9\beta^4 \end{array} \right)}{16(2\zeta_e + \beta) (12\zeta_e^2 + 12\beta\zeta_e + 4 + 3\beta^2)^2}. \quad (26)$$

Equation (26) is a sextic equation for ζ_e . Solving the equation we find ζ_e and the damping ratio of the dampers is determined from (20).

We can further simplify the optimal solution with the remark that ζ_e is usually very small compared to 1. It is possible to ignore the terms higher than 2 of ζ_e , to reduce the equation (26) to:

$$\zeta_e = \frac{3\phi_0^2}{64(2\zeta_e + \beta)} \Rightarrow \zeta_e = \frac{\sqrt{16\beta^2 + 6\phi_0^2} - 4\beta}{16}. \quad (27)$$

And the optimal damping ratio is:

$$\zeta_{\text{opt}} = 2\zeta_e + \beta = \frac{\sqrt{16\beta^2 + 6\phi_0^2} + 4\beta}{8}. \quad (28)$$

In brief, we have determined the optimal parameters of dampers in the case of a combination of proportional feedback control with the use of dampers. The analytical solution is determined by (19) and (28).

4. Numerical simulation

Numerical calculation is performed in the non-dimensional crane model (6). In this section, we will simulate two cases: the case of inactive crane and the crane in operation to compare the effect of reducing vibration. In the case of an inactive crane, the trolley's movement is due to the feedback control signal:

$$\dot{x}_n = \beta\phi. \quad (29)$$

In the case of the crane in operation, the trolley's movement is due to the feedback control signal and the crane's operator:

$$\dot{x}_n = v_r + \beta\phi, \quad (30)$$

where v_r is the velocity determined by the crane's operator. The vibration of the payload, when the crane is in operation, depends on the operating conditions. Here, for demonstration, we consider the case of the simplest operation but causes for large vibrations. The simple case is considered with the triangular velocity control signal (Fig. 2). The operator speeds up the trolley with a constant acceleration. When it reaches a half of the travel, the operator reduces the trolley speed with

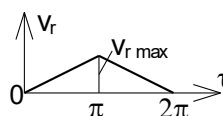


Fig. 2. The velocity of the trolley is made by the operator

the same constant acceleration. The velocity will decrease to zero when the trolley reaches the required travel. The operating acceleration is assumed to have the form:

$$\dot{v}_r = \begin{cases} a_m & 0 \leq \tau < \pi, \\ -a_m & \pi \leq \tau < 2\pi, \\ 0 & \tau \geq 2\pi. \end{cases} \quad (31)$$

a_m is the dimensionless acceleration and will be altered for investigation.

Input values used in the numerical computation are taken as follows: the radial spring-damper is designed for the large vibration angle up to 30° , i.e., the angle φ_0 is chosen of $\pi/6$ in (28). The results of r_{opt} and ζ_{opt} are shown in Table 2.

Table 2.

Optimal values of r and ζ with angle of $\pi/6$

| Parameter | | Value |
|----------------------|----------------|--------|
| r_{opt} | | 2 |
| ζ_{opt} | $\beta = 0.05$ | 0.1873 |
| | $\beta = 0.1$ | 0.2179 |

For convenience, we denote the simulation cases in Table 3.

Table 3.

The simulation cases

| Notation | C1 | C2 | C3 | C4 |
|----------------------|----|-----|-----|-----|
| Feedback control | No | Yes | No | Yes |
| Radial spring-damper | No | No | Yes | Yes |

4.1. Case of inactive crane

First, we consider the case of payload oscillation caused by the initial angle without the trolley motion.

The swing angles are shown in Figs. 3–4 with various cases of initial angle and feedback control gain.

We also calculate the remaining oscillation angle after 4 periods. The comparison results are shown in Table 4.

The results give the following remarks:

- In case 3 (with damper, without active control), the performance is better if the initial angle is larger (60.5% in comparison with 43.1%).
- In case 2 (without damper, with active control), the performance does not depend on the initial angle, but on the control gain β . The larger control gain gives better performance.
- Case 4 combining two methods is indeed better than the cases of each separate method. That means using the combination still allows for good performance but does not make too serious a conflict with the crane operator.

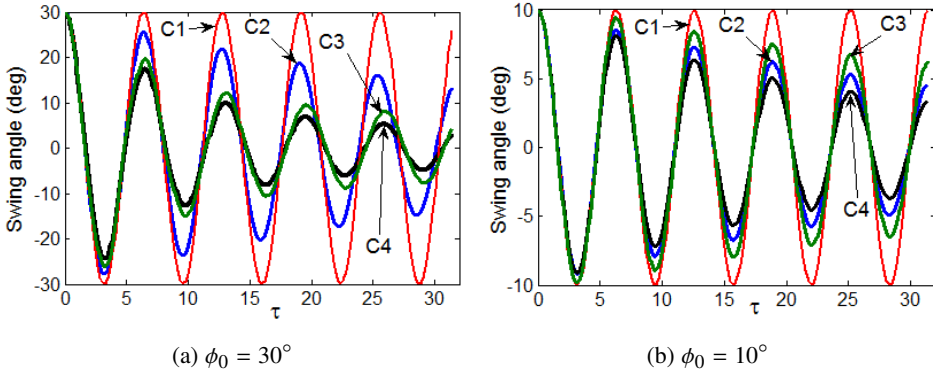


Fig. 3. Swing angle versus normalized time for $\beta = 0.05$ and different ϕ_0

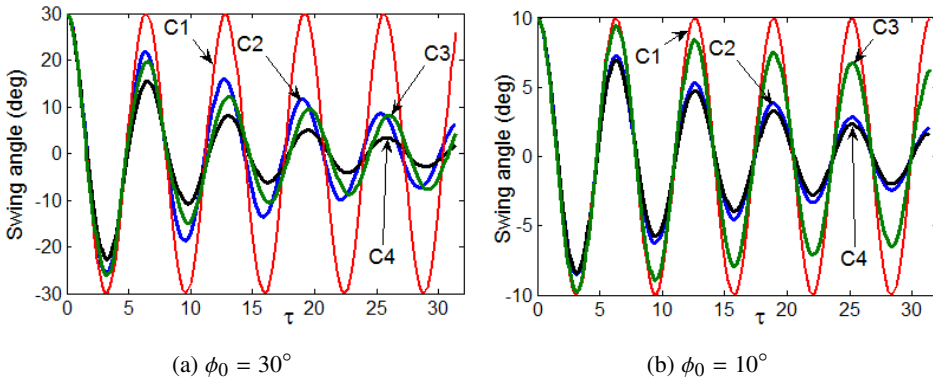


Fig. 4. Swing angle versus normalized time for $\beta = 0.1$ and different ϕ_0

Table 4.

Maximum angle (degree) after 4 periods (percentile beside shows the reduction of swinging)

| Case | C1 | C2 | C3 | C4 |
|-----------------------------------|---------|---------------|---------------|--------------|
| $\phi_0 = 30^\circ, \beta = 0.05$ | 30 (0%) | 15.94 (46.9%) | 11.85 (60.5%) | 7.03 (76.6%) |
| $\phi_0 = 10^\circ, \beta = 0.05$ | 10 (0%) | 5.31 (46.9%) | 5.68 (43.1%) | 3.55 (64.5%) |
| $\phi_0 = 30^\circ, \beta = 0.1$ | 30 (0%) | 8.52 (71.6%) | 11.85 (60.5%) | 4.08 (86.4%) |
| $\phi_0 = 10^\circ, \beta = 0.1$ | 10 (0%) | 2.84 (71.6%) | 5.68 (43.1%) | 2.09 (79.1%) |

4.2. Case of the crane in operation

In the case of the crane in operation, the trolley's movement is due to the feedback control signal and operator. The velocity of the trolley is taken from (30). The comparison results are shown in Figs. 5–6 and Table 5.

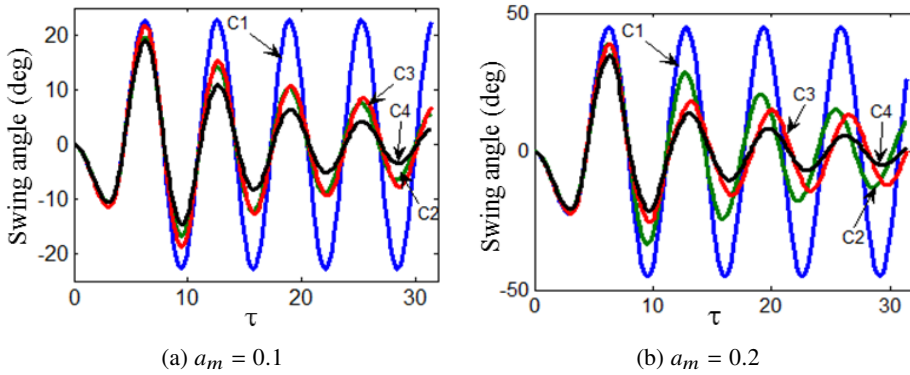


Fig. 5. Swing angle versus normalized time for $\beta = 0.05$ and different a_m

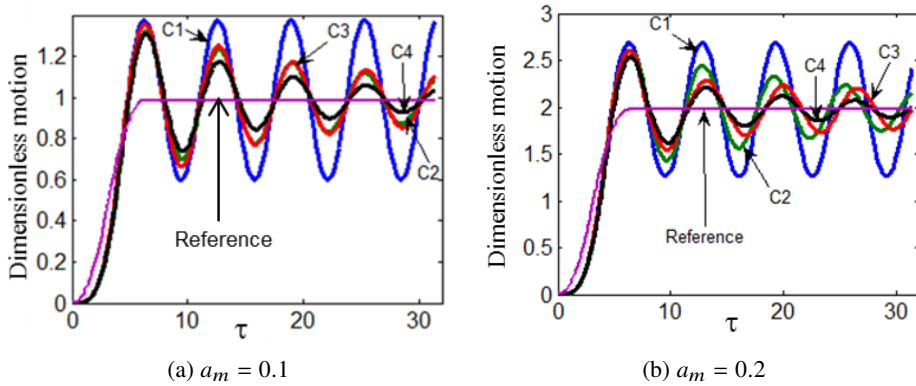


Fig. 6. The horizontal motion of the payload versus normalized time for $\beta = 0.1$ and different a_m

Table 5.

Maximum angle (degree) after 4 periods (percentile beside shows the reduction of swinging)

| Case | C1 | C2 | C3 | C4 |
|--------------------------|------------|---------------|---------------|--------------|
| $a_m = 0.1, \beta = 0.1$ | 22.85 (0%) | 7.64 (66.6%) | 8.43 (63.1%) | 4.18 (81.7%) |
| $a_m = 0.2, \beta = 0.1$ | 45.09 (0%) | 15.20 (66.3%) | 13.23 (70.7%) | 5.76 (87.2%) |

The results show that:

- When acceleration is increased, the sway angle also increases. Since the spring-damper efficiency increases with sway angle, cases 3 and 4 have better performance in the case of large acceleration.
- Case 4 that combines both methods still gives better efficiency than every single method.
- The horizontal motion of the payload in case 4 is the closest to the desired movement. That affirms the combined method, which reduces vibrations well, while still ensuring the payload following the desired trajectory.

4.3. The robustness of the proposed method

In the above calculations, we simulated the system with certain parameters. These parameters can be varied, such as the cable's length, the payload mass, and the fabrication error of the radial spring-damper k and c or error of external disturbances such as wind. To evaluate the effectiveness of the proposed method, in this section, we consider the 20% error of the above parameters in the simulation. Simulation results are shown in Figs. 7–9. Comparing Fig. 5a with Figs. 7a, 8a, and Table 5 with Tables 6, 7 we see that when the parameters change, the cases 3 and 4 using spring-damper have reduced efficiency (36.44% in comparison with 63.1%; 71.37% in comparison with 81.7%). This is due to non-optimal parameters of the spring-damper. However, case 4 still gives better performance than the rest. This proves the robustness of the proposed method.

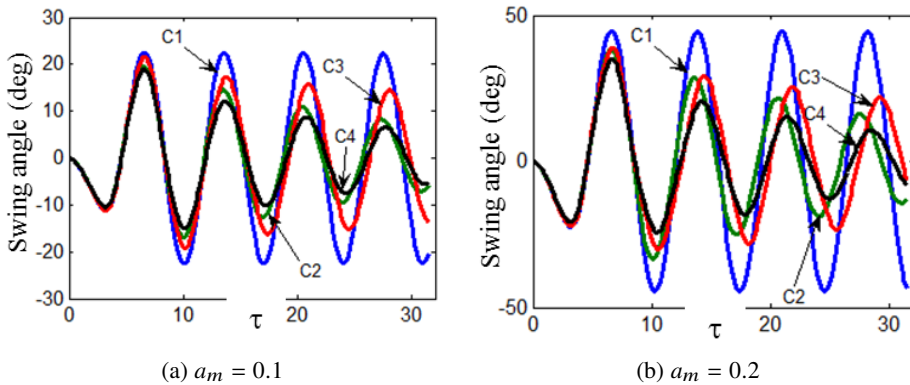


Fig. 7. Swing angle versus normalized time for $\beta = 0.1$ and different a_m . Case l, m are increased by 20%; k, c are reduced by 20%

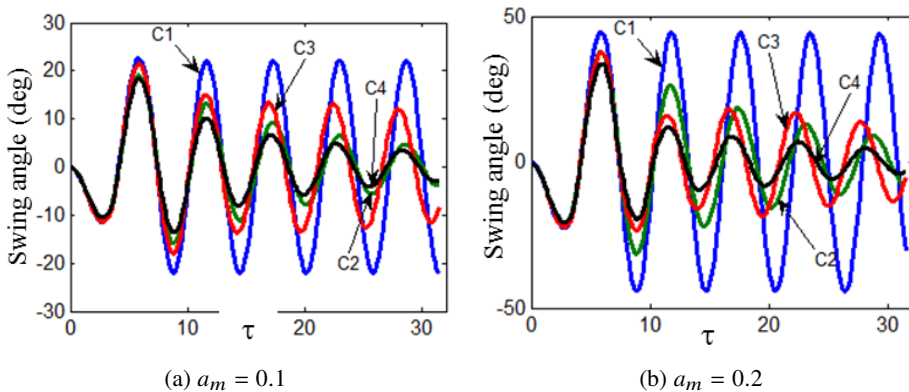


Fig. 8. Swing angle versus normalized time for $\beta = 0.1$ and different a_m . Case l, m are reduced by 20%; k, c are increased by 20%

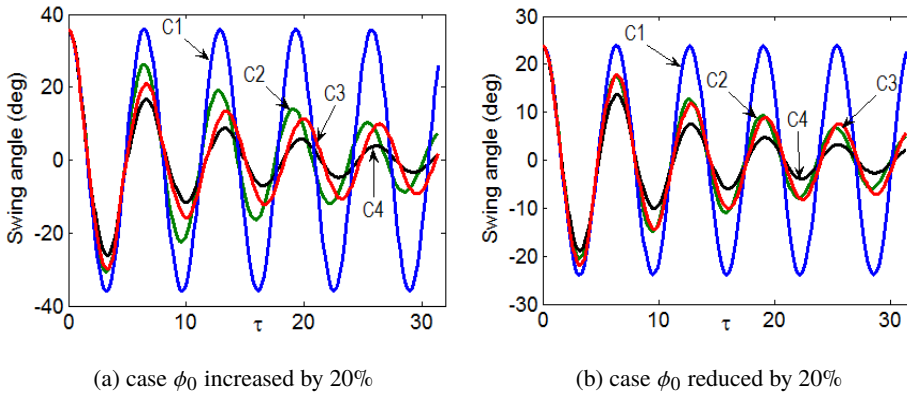


Fig. 9. Swing angle versus normalized time for $\beta = 0.1$ and different case ϕ_0

Table 6.

Maximum angle (degree) after 4 periods (percentile beside shows the reduction of swinging)
Case l, m are increased by 20%; k, c are reduced by 20%

| Case | C1 | C2 | C3 | C4 |
|--------------------------|------------|----------------|----------------|----------------|
| $a_m = 0.1, \beta = 0.1$ | 22.53 (0%) | 8.24 (63.42%) | 14.32 (36.44%) | 6.45 (71.37%) |
| $a_m = 0.2, \beta = 0.1$ | 44.57 (0%) | 16.31 (63.41%) | 18.29 (58.96%) | 10.62 (76.17%) |

Table 7.

Maximum angle (degree) after 4 periods (percentile beside shows the reduction of swinging)
Case l, m are reduced by 20%; k, c are increased by 20%

| Case | C1 | C2 | C3 | C4 |
|--------------------------|------------|----------------|----------------|---------------|
| $a_m = 0.1, \beta = 0.1$ | 22.12 (0%) | 5.48 (75.23%) | 13.76 (37.79%) | 4.50 (79.66%) |
| $a_m = 0.2, \beta = 0.1$ | 44.27 (0%) | 10.94 (75.29%) | 20.37 (53.98%) | 7.55 (82.95%) |

5. Verification simulation

To demonstrate the effectiveness of the proposed combination method, a 2D crane model is simulated independently using the software RECURDYN [17]. The model's parameters are as follows: $l = 0.9$ m, payload mass: $m_P = 1.5$ kg, spring's stiffness k , and damper's coefficient c are taken from Table 1 with r (defined in (18)) is equal to 2, ζ (defined in (19)) is equal to 0.2. The 2D crane model in RECURDYN is shown in Fig. 10.

To induce the initial motion of the payload for the case of an inactive crane, we assume that the payload has an initial velocity v_0 (this initial velocity can be the result of a short and large wind gust). In the case of the crane in operation, the acceleration of the trolley a is still taken from (30). The commands to control the trolley are done with the help of Matlab Simulink. The simulation results are shown in Figs. 11–14.

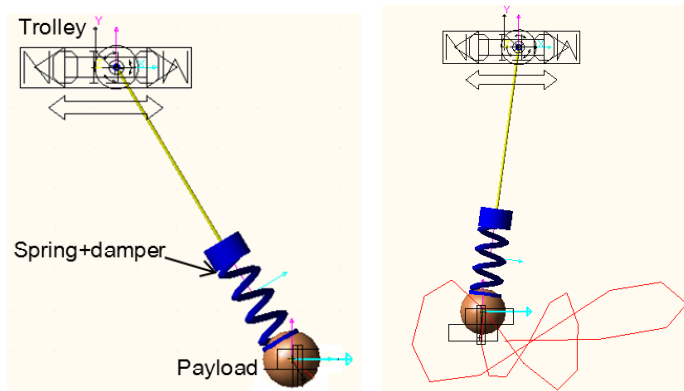


Fig. 10. 2D crane model in RECURDYN

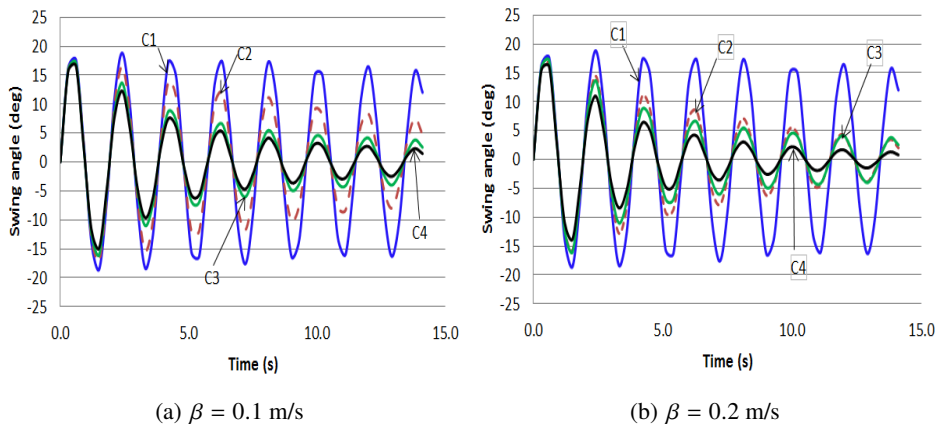


Fig. 11. Swing angle of payload for $v_0 = 1$ m/s and different β

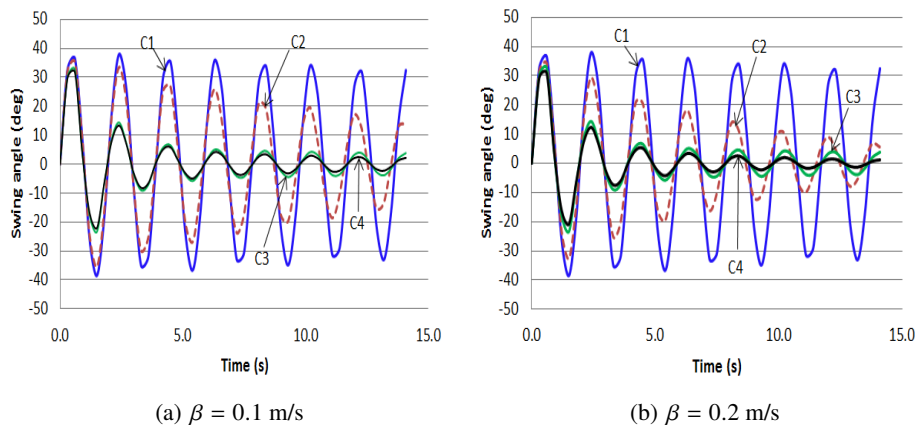
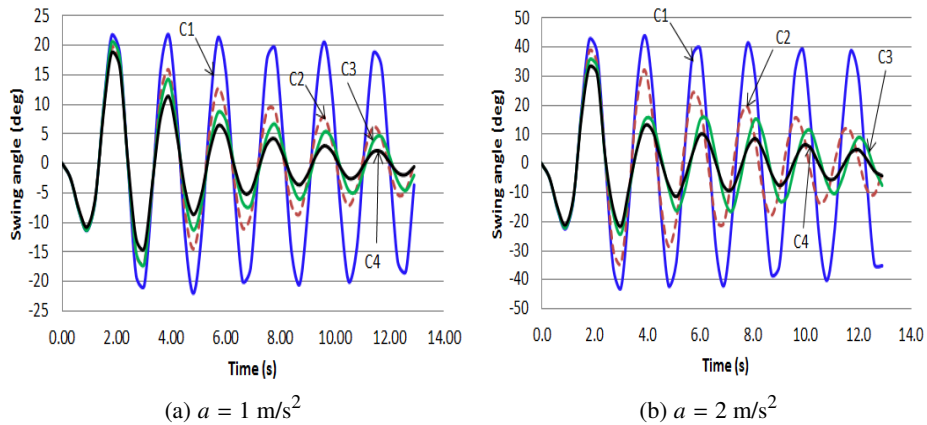
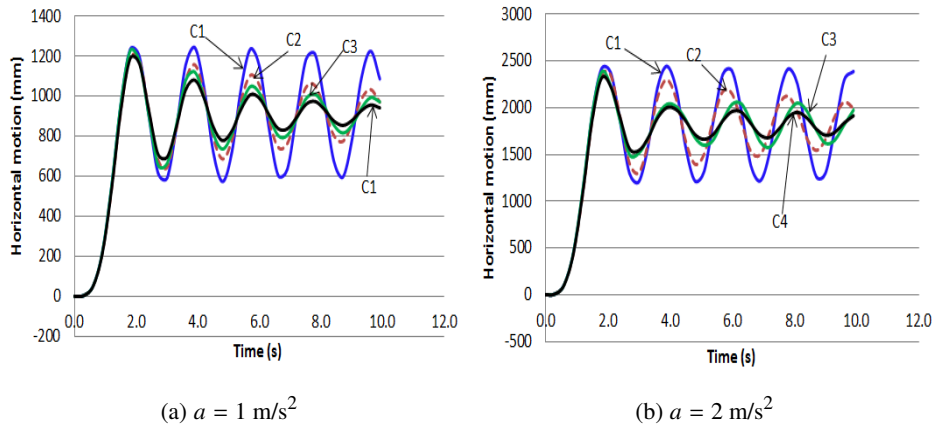


Fig. 12. Swing angle of payload for $v_0 = 2$ m/s and different β

Fig. 13. Swing angle of payload for $\beta = 0.2 \text{ m/s}$ and different a Fig. 14. Horizontal motion of payload for $\beta = 0.2 \text{ m/s}$ and different a

The results show that: when further simulated by independent software RECURDYN and the simulation parameters are physical parameters ($l = 0.9 \text{ m}$, $m_P = 1.5 \text{ kg}$, . . .), case 4 that combines both methods still gives better efficiency than every single method in all cases. Once again, it proves the effectiveness of the proposed method.

6. Conclusion

This paper proposes the combination of proportional feedback control with the use of dampers to control the swaying of the crane payload. The dampers and low-authority feedback controller simultaneously eliminate payload oscillation caused by initial conditions and operator's commands. The combined dampers and low-authority feedback control architecture produced a robust control effect that reduced

the unwanted oscillation of the payload. Numerical calculations and simulations were used to verify the effectiveness of the proposed method, for various cases of initial angle, initial velocity, drive acceleration, and control gain. Besides, the optimal parameters of the spring-damper system have been derived.

Manuscript received by Editorial Board, January 17, 2021;
final version, June 11, 2021.

References

- [1] D. Kim and Y. Park. Tracking control in x-y plane of an offshore container crane. *Journal of Vibration and Control*, 23(3):469–483, 2017. doi: [10.1177/1077546315581091](https://doi.org/10.1177/1077546315581091).
- [2] D.H. Kim and J.W.Lee. Model-based PID control of a crane spreader by four auxiliary cables. *Proceedings of the Institution of Mechanical Engineers, Part C: Journal of Mechanical Engineering Science*, 220(8):1151–1165, 2006. doi: [10.1243/09544062JMES120](https://doi.org/10.1243/09544062JMES120).
- [3] N. Uchiyama. Robust control of rotary crane by partial-state feedback with integrator. *Mechatronics*, 19(8):1294–1302, 2009. doi: [10.1016/j.mechatronics.2009.08.007](https://doi.org/10.1016/j.mechatronics.2009.08.007).
- [4] J. Smoczek. Fuzzy crane control with sensorless payload deflection feedback for vibration reduction. *Mechanical Systems and Signal Processing*, 46(1):70–81, 2014. doi: [10.1016/j.ymsp.2013.12.012](https://doi.org/10.1016/j.ymsp.2013.12.012).
- [5] M. Zhang, X. Ma, X. Rong, X. Tian, and Y. Li. Adaptive tracking control for double-pendulum overhead cranes subject to tracking error limitation, parametric uncertainties and external disturbances. *Mechanical Systems and Signal Processing* 76-77:15–32, 2016. doi: [10.1016/j.ymsp.2016.02.013](https://doi.org/10.1016/j.ymsp.2016.02.013).
- [6] L.D. Viet and K.T. Nguyen. Combination of input shaping and radial spring-damper to reduce tridirectional vibration of crane payload. *Mechanical Systems and Signal Processing*, 116:310–321, 2019. doi: [10.1016/j.ymsp.2018.06.056](https://doi.org/10.1016/j.ymsp.2018.06.056).
- [7] L.D. Viet and Y. Park. A cable-passive damper system for sway and skew motion control of a crane spreader. *Shock and Vibration*, 2015:507549, 2015. doi: [10.1155/2015/507549](https://doi.org/10.1155/2015/507549).
- [8] L.D. Viet. Crane sway reduction using Coriolis force produced by radial spring and damper. *Journal of Mechanical Science and Technology*, 29(3):973–979, 2015. doi: [10.1007/s12206-015-0211-1](https://doi.org/10.1007/s12206-015-0211-1).
- [9] J. Vaughan, E. Maleki, and W. Singhose. Advantages of using command shaping over feedback for crane control. *Proceedings of the 2010 American Control Conference*, pages 2308–2313, 2010. doi: [10.1109/ACC.2010.5530548](https://doi.org/10.1109/ACC.2010.5530548).
- [10] J. Vaughan, A. Yano, and W. Singhose. Comparison of robust input shapers. *Journal of Sound and Vibration*, 315(4-5):797–815, 2008. doi: [10.1016/j.jsv.2008.02.032](https://doi.org/10.1016/j.jsv.2008.02.032).
- [11] W. Singhose. Command shaping for flexible systems: A review of the first 50 years. *International Journal of Precision Engineering and Manufacturing*, 10(4):153–168, 2009. doi: [10.1007/s12541-009-0084-2](https://doi.org/10.1007/s12541-009-0084-2).
- [12] J. Lawrence and W. Singhose. Command shaping slewing motions for tower cranes. *Journal of Vibration and Acoustics*, 132(1):011002, 2010. doi: [10.1115/1.3025845](https://doi.org/10.1115/1.3025845).
- [13] D. Blackburn, W. Singhose, J. Kitchen, V. Patrangenaru, J. Lawrence, K. Tatsuaki, and A. Taura. Command shaping for nonlinear crane dynamics. *Journal of Vibration and Control*, 16(4):477–501, 2010. doi: [10.1177/1077546309106142](https://doi.org/10.1177/1077546309106142).
- [14] J. Huang, E. Maleki, and W. Singhose. Dynamics and swing control of mobile boom cranes subject to wind disturbances, *IET Control Theory and Applications*, 7(9):1187–1195, 2013. doi: [10.1049/iet-cta.2012.0957](https://doi.org/10.1049/iet-cta.2012.0957).

- [15] R. Schmidt, N. Barry, and J. Vaughan. Tracking of a target payload via a combination of input shaping and feedback control. *IFAC-PapersOnLine*, 48(12):141–146, 2015. doi: [10.1016/j.ifacol.2015.09.367](https://doi.org/10.1016/j.ifacol.2015.09.367).
- [16] N.D. Anh, H. Matsuhisa, L.D. Viet, and M. Yasuda. Vibration control of an inverted pendulum type structure by passive mass-spring-pendulum dynamic vibration absorber. *Journal of Sound and Vibration*, 307(1-2):187–201, 2007. doi: [10.1016/j.jsv.2007.06.060](https://doi.org/10.1016/j.jsv.2007.06.060).
- [17] Function Bay Inc., <http://www.functionbay.co.kr/>, last checked 27 May 2020.